Georegistration of Airborne Hyperspectral Image Data

Changno Lee and James Bethel

***Abstract*—A suite of geometric sensor and platform modeling tools has been developed which have achieved consistent subpixel accuracy in orthorectification experiments. Aircraft platforms in turbulent atmospheric conditions present unique challenges and have required creative modeling approaches. The geometric relationship between an image point and a ground object has been modeled by rigorous photogrammetric methods. First and second order Gauss-Markov processes have been used to estimate the platform trajectory. These methods have been successfully applied to HYDICE and HyMap data sets. The most important contributors to the subpixel rectification accuracy have been the first order Gauss-Markov model with control linear features.**

***Index Terms*—Airborne hyperspectral imagery, georegistration, linear feature, rectification.**

I. Introduction

HYPERSPECTRAL data analysis has repeatedly been shown to yield high quality thematic maps in urban areas. Airborne hyperspectral imagery has high spatial resolution compared to traditional spaceborne hyperspectral imagery. Therefore, airborne sensors are suitable for cartographic applications where accurate geopositioning is critical. However, aircraft-mounted scanners are subject to atmospheric turbulence during their flight which can lead to severe image distortions in the raw imagery.

The estimation of sensor position and attitude parameters in cases of near continuous data capture becomes very closely related to the problem of platform trajectory estimation. Orientation parameters for pushbroom sensors in low earth orbit can be successfully modeled as polynomial functions of time [11] or as spline functions of time [4]. For pushbroom sensors on airborne platforms these strategies are less successful, although having a multiline focal plane can stabilize the result [5]. Breuer [2] classifies geometric modeling of scanner imagery into 1) nonparametric methods or "rubber sheeting," 2) parametric methods as described above, and 3) hybrid or mixed methods. A further subdivision of the parametric method can be made depending on whether the estimated parameters are considered deterministic or random [8]. A recent enhancement of the nonparametric method, referred to as the rational function model [12] permits the projection of three-dimensional (3-D) object points into two-dimensional (2-D) imagery rather than the more simplistic case of 2-D object points into 2-D imagery. In the aforementioned models, it is important to note that each ground point is imaged only once during the image capture. This contrasts with video or motion imagery wherein each ground point may be imaged onto many successive image frames, permitting the use of optical flow techniques to aid in platform trajectory determination [10]. Radiometric and sensor architecture considerations have thus far prevented any hyperspectral sensor from operating in this fast framing mode.

The relation between image point and ground object can be modeled by rigorous photogrammetric methods [1]. In photogrammetric sensor modeling, each scan line is modeled as a frame image. Therefore, a different set of values for the exterior orientation parameters needs to be determined for each scan line. Then, platform modeling is required to estimate the platform trajectory. In this case, the platform model should be flexible to accommodate abrupt changes of the orientation elements [7].

II. Hyperspectral Imagery

A. HYDICE Data

The hyperspectral digital imagery collection experiment (HYDICE) sensor is an airborne pushbroom imaging spectrometer with 210 spectral channels ranging from 0.4 μm to 2.5 μm. With a 0.5 mrad instantaneous field of view (IFOV), the ground sample distance (GSD) varies from 0.75 to 3.75 m depending on the platform altitude above ground.

In addition to image data, support information is available for each scan line. These support data consist of Inertial navigation system (INS) data, global positioning system (GPS) data, flight stabilization subsystem (FSS) pointing knowledge, and HYDICE engineering data. These data are updated to reflect current information for each scan line. However, some fields can't be updated as frequently as the frame time, in which case the same values are repeated until updated information is available (e.g., GPS data).

HYDICE image was collected over the urban area of Fort Hood, TX, in October 1995 (Fig. 1). Its GSD and flying height are 2.2 m and about 4430 m, respectively. As can be seen from Fig. 1, straight roads in the direction of flight can be severely wavy.

B. HyMap Data

The HyMap sensor is an airborne whiskbroom imaging spectrometer with 126 spectral bands across the reflective

Manuscript received September 26, 2000; revised January 9, 2001. This work was supported by the U.S. Army Research Office (ARO) through a Multidisciplinary University Research Initiative (MURI) Project "Rapid and Affordable Generation of Terrain and Detailed Urban Feature Data" under Grant DAAH04-96-1-0444.

The authors are with the School of Civil Engineering, Purdue University, West Lafayette, IN 47907 USA.

Publisher Item Identifier S 0196-2892(01)05500-0.

Fig. 1. HYDICE Imagery Data Set (Fort Hood).

solar wavelength region of 0.45–2.5 nm with contiguous spectral coverage. HyMap collects ground surface information continuously by sweeping from side to side as the platform moves forward. Its ground sample distance varies from 3 m to 10 m depending on the platform altitude above ground.

The HyMap system also provides geolocation and image geocoding achieved by DGPS and an integrated IMU (inertial monitoring unit). UTM coordinates are available for each original image pixel, and six exterior orientation parameters are supported for each scan line. The HyMap data was collected over the Purdue Campus in West Lafayette, Indiana during September, 1999 (Fig. 2). The flying height and GSD were about 1600 m and 3.2 m, respectively.

Fig. 2. HyMap imagery data set (Purdue University, West Lafayette, IN).

III. Geometric Model

The objective of geometric modeling is to relate pixels in an image to coordinates in a ground coordinate system. Sensor types for hyperspectral imagery can be divided into two groups, pushbroom and whiskbroom.

In pushbroom imaging systems, each scan line is considered as a framelet. Therefore, the photogrammetric collinearity condition can be applied within each line of the pushbroom images as the geometric model.

Strictly speaking, a whiskbroom scanner sweeps multiple pixels across the flight path. We will consider the limiting case where only a single pixel is swept across track. Therefore, each image pixel, which is collected at a different time, requires its own set of six exterior orientation elements. To relieve this indeterminate situation, it is assumed that the time to complete one scan line is small enough to consider one exposure station for each scan line. Then, each scan line of a whiskbroom image can be modeled as a panoramic image, instead of a framelet as used in the pushbroom model. Modeling from line to line remains the same for both imaging modes.

A. Pushbroom Sensor

The geometric relationship between the ground point and image point of pushbroom imagery can be expressed by the collinearity condition for a given scan line as in Fig. 3. For the image coordinate system, we define the origin as the perspective center, the x-axis as the flight direction, the z-axis normal to the linear array (up) through the perspective center, and the y-axis as necessary to achieve a right-handed Cartesian system. The relationship between the ground coordinates and corresponding image coordinates can then be expressed as in (1) and (2) [5]

$$F_x = x + fl\frac{U}{W} = 0 \tag{1}$$

$$F_y = y + fl\frac{V}{W} = 0 \tag{2}$$

where

$$\begin{bmatrix} U \\ V \\ W \end{bmatrix} = M \begin{bmatrix} X - X_L \\ Y - Y_L \\ Z - Z_L \end{bmatrix} \tag{3}$$

where

x, y	coordinates of image point in image coordinate system;
X, Y, Z	coordinates of object point in ground coordinate system;
X_L, Y_L, Z_L	coordinates of instantaneous perspective center in ground coordinate system;
M	3×3 orthogonal rotation matrix from the ground coordinate system to image coordinate system;
fl	calibrated focal length.

From (1) and (2), notice that the six exterior orientation (EO) parameters, consisting of three coordinates (X_L, Y_L, Z_L) of the instantaneous perspective center position and three independent

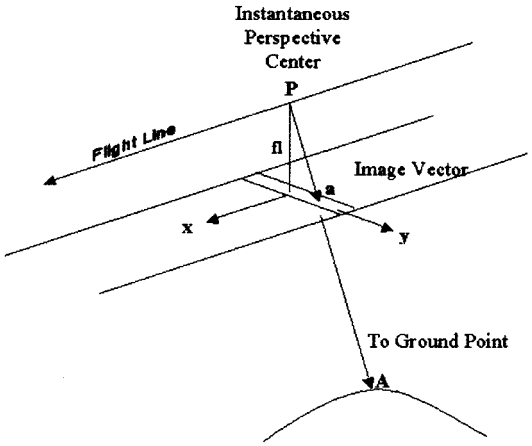

Fig. 3. Collinearity condition.

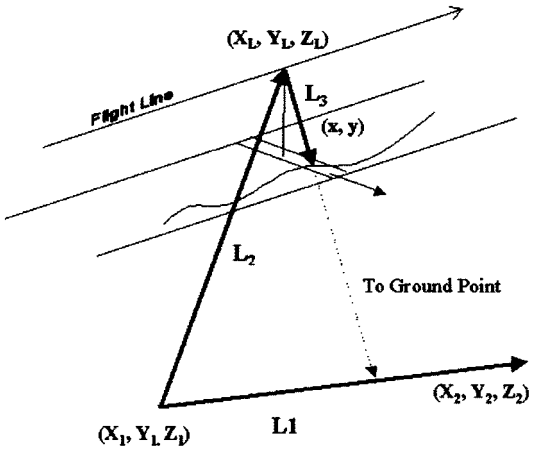

Fig. 4. Control line model.

rotational angles $(\omega, \varphi, \kappa)$ have different values for each scan line.

Linear features offer some advantages over control points in their use as control features. Unlike frame imagery, straight linear features on the ground may appear wavy in the raw scanner imagery. This deformation of the linear features provides detailed information about the platform trajectory so that changes in the sensor orientation can be detected and estimated. Linear features such as building edges and road boundaries are abundant in urban areas and are often easy to extract using semi-automated tools. Although the term linear feature encompasses any continuous feature with a negligible width and includes such parameterizations as splines, we concern ourselves with the special case of straight-line features in the remainder of the paper.

The image vector $L3$ in Fig. 4, formed by the image of a linear feature in a given scan line and transformed to the ground coordinate system, is in a plane that is defined by three points, i.e., two end points of the linear feature in the ground space and the position of the instantaneous perspective center. Therefore, the determinant of the three vectors in Fig. 4 should be equal to zero. The control line model can be expressed as follows:

$$F_P = |L1\ L2\ L3| = 0 \tag{4}$$

TABLE I
COMPARISON BETWEEN THE FIRST AND SECOND GAUSS–MARKOV MODELS

Type of models	Check point RMS (m)			
	Fort Hood GSD = 2.2 m		Purdue GSD = 3.2 m	
	ΔX	ΔY	ΔX	ΔY
1st order GM	1.50	1.35	1.57	1.49
2nd order GM	1.66	1.26	2.02	2.84
Polynomial	2.37	8.24	3.35	2.81

TABLE II
USE OF GPS/INS WITH CONTROL POINT DATA

Type of models	Check point RMS (m)			
	Fort Hood GSD = 2.2 m		Purdue GSD = 3.2 m	
	ΔX	ΔY	ΔX	ΔY
Model 1	38.10	2.45	3.68	5.22
Model 2	1.57	1.13	2.22	1.70
Model 3	1.58	1.12	1.75	1.61

where

$$L1 = [X_2 - X_1 \quad Y_2 - Y_1 \quad Z_2 - Z_1]^{\mathrm{T}}$$
$$L2 = [X_L - X_1 \quad Y_L - Y_1 \quad Z_L - Z_1]^{\mathrm{T}}$$
$$L3 = M^{\mathrm{T}}[X \quad Y \quad -fl]^{\mathrm{T}}.$$

Another possible line model is the parametric form. In this form, each coordinate (X, Y, Z) of a point along a line is expressed in terms of the independent parameter u associated with the accumulated length along the line between two end points corresponding to u equals to 0 and 1, respectively [7].

The parametric model can be used to model general linear features such as splines. However, the parametric model requires an additional line parameter (u) for each point on a line, and the total number of parameters is very large. Therefore, this parametric model needs additional processing to reduce the required matrix size and will not be considered in this paper.

B. Whiskbroom Sensor

A whiskbroom sensor collects each pixel of data at a different time. Therefore, each pixel can be considered as a unique frame image. However, as stated earlier, to reduce the number of orientation parameters we have assumed that all of the pixels in a given line are collected at the same time. First, the pixel position error from panoramic effects should be corrected. Then, the geometric relationship between the image points and the ground points can be expressed as in a pushbroom sensor.

C. Gauss-Markov Process

In the observation (1), (2), and (4), a different set of six elements of EO must be estimated for each scan line. Consequently, so many parameters may need to be solved for that the problem

Fig. 5. Ortho-rectified Image (Fort Hood).

becomes impractical due to the large number of required control points. This situation can be addressed by using *a priori* information about the behavior of the platform. Even though an airborne hyperspectral sensor may encounter severe air turbulence during its flight, a stabilization platform can dampen the attitude excursions. The time interval between two adjacent lines is very short. Therefore each of the six exterior parameters will change slowly between successive lines. Also each EO parameter in a given scan line will be highly correlated to that in the adjacent scan lines. Based on these properties, the first and second Gauss–Markov process can be derived for each of the six EO parameters [7].

By assuming the six EO parameters for each scan line are being driven by a stationary Gauss-Markov process, stochastic relationships from the process can be integrated with the underdetermined functional model. By using Kalman smoothing, the measurements and the statistical properties of the process at each line are used to form condition equations, and the adjustment is augmented on a line by line basis [3]. In this approach, the state vector consists of six EO parameters for the first order Gauss–Markov model. For the second order Gauss–Markov, the state vector consists of 12 parameters, six EO parameters and six velocities of EO parameters. Therefore, this approach requires much less computational time compared to other Kalman filtering processes for the sensor orientation.

IV. Experiments

A. Control and Check Data

To determine the parameters of the sensor model, we need both image coordinates and ground coordinates for control data and the performance is evaluated by using separate check data. The ground coordinates are commonly obtained from a conventional field survey or a GPS survey. In our data sets, however, the ground coordinates of point data and the end points of the lines are obtained from higher accuracy, triangulated aerial frame photography.

A total of 232 points were extracted for the Fort Hood area. The same 116 check points were used in all of the experiments, leaving up to 116 control points available for the HYDICE restitution. For the Purdue campus area, a total of 34 points were extracted from the frame photography on a digital photogrammetric workstation. The same eight check points were used in all of the experiments, with the other 26 control points available for the HyMap restitution.

Fig. 6. Ortho-rectified Image (Purdue Campus).

The extracted straight lines generally fell into two categories, e.g., road boundaries and building sides. For the Fort Hood area, 50 straight linear features were extracted from the HYDICE imagery. Similarly, 20 lines were extracted from the Purdue campus area.

B. Post–Adjustment Analysis

The purpose of this section is to compare the accuracy obtained from the restitution of hyperspectral imagery using different platform models. In order to quantify the performance of each model, we examine the residuals of check points. Since we have only single image coverage, the Z-coordinate must be fixed to its known value. This does not imply a flat terrain assumption, but that the various Z coordinates of points and features are indeterminate using a single image.

For the comparison of performance, a third-order polynomial sensor model is used to transform between object and image space. This type of sensor model doesn't require physical sensor information. Therefore, it can be used for any sensor type without physical sensor information.

The RMS residuals of check points are summarized for both data sets (Table I). Gauss–Markov models showed much better results compared to the polynomial model.

C. Use of GPS and INS Data

By using onboard GPS and INS data, airborne scanner imagery can be rectified without control points. In this section, the use of GPS and INS data is investigated with various conditions. First, sensor orientation parameters are recovered using only GPS and INS data (Model 1). Next, control point information is used with a third-order polynomial math model to estimate the differences between true angular values and INS data while sensor positions were fixed to GPS data (Model 2). Finally, all the differences between true value and GPS/INS data were estimated using the third order polynomial math model and the ground control point information (Model 3).

As in previous experiments, the same check points were used to examine the performance of each model. Table II shows check point RMS residuals for different models with only control points. Linear features were not helpful for the estimation of parameters when GPS/INS data were added. The performance of Model 3 is similar to that of the first order Gauss-Markov model. However implementation is simpler because the number of parameters is much less than that for the Gauss-Markov model, and control lines are not needed.

D. Rectification

In addition to the numerical results of experiments, the performance of the proposed rectification model was presented visually by orthorectified images (Figs. 5 and 6). For each grid point in ground space, the corresponding image pixel position was computed based on the collinearity equation with the first order Gauss-Markov platform model, and the pixel brightness value was determined by nearest neighbor resampling to preserve the absolute radiometric properties of the original image. Notice the straightness of the roads in the orthorectified images compared to the visible departures from straightness in the raw images.

V. Conclusions

Based on checkpoint RMS error, the first order Gauss-Markov model showed the best performance for both data sets. The Gauss–Markov model is flexible in the sense that it can accommodate abrupt changes in the position and orientation of the sensor aboard the aircraft. This flexibility contributes to the performance of the model by using straight linear features as control data. For the whiskbroom image (Purdue data), the registration accuracy was about a half pixel and the corresponding ortho-rectified image did not show any discontinuity. Therefore, the time difference within a scan line should be small enough for the stated assumption of whiskbroom imagery.

GPS/INS data were very useful when control point information was combined for the estimation. This approach showed similar performance compared to the first order Gauss-Markov model and the process was much simpler with less ground control information.

References

[1] J. Bethel, C. Lee, and D. Landgrebe, "Geometric registration and classification of hyperspectral airborne pushbroom data," *Int. Arch. Photogramm. Remote Sensing*, pt. B7, vol. 33, pp. 183–188, 2000.

[2] M. Breuer and J. Albertz, "Geometric correction of airborne whiskbroom scanner imagery using hybrid auxiliary data," *Int. Arch. Photogramm. Remote Sensing*, pt. B3, vol. 33, pp. 93–100, 2000.

[3] R. G. Brown and P. Y. C. Hwang, *Introduction to Random Signals and Applied Kalman Filtering*, 3rd ed. New York: Wiley, 1997.

[4] A. de Haan, "Contribution of the Politecnico di Milano to the OEEPE test on triangulation with SPOT data," in *Test of Triangulation of SPOT Data, Official Publication no. 26*. Frankfurt am Main, Germany: Eur. Org. Experimental Photogramm. Res., 1991, pp. 93–107.

[5] H. Ebner and F. Muller, "Processing of digital three-line imagery using a generalized model for combined point determination," *Photogrammetria*, vol. 41, pp. 173–182, 1987.

[6] A. Gelb, *Applied Optimal Estimation*. Cambridge, MA: Mass. Inst. Technol., 1974.

[7] C. Lee, H. Theiss, J. Bethel, and E. Mikhail, "Rigorous mathematical modeling of airborne pushbroom imaging systems," *Photogramm. Eng. Remote Sensing*, vol. 66, pp. 385–392, Apr. 2000.

[8] J. Mendel, *Lessons in Digital Estimation Theory*. Englewood Cliffs, NJ: Prentice-Hall, 1987.

[9] F. H. Moffitt and E. M. Mikhail, *Photogrammetry*, 3rd ed. New York: Harper & Row, 1980.

[10] Y. Oshman and B. Menis, "Maximum a posteriori image registration/motion estimation," *J. Guidance, Contr., Dynam.*, vol. 17, pp. 1115–1123, Sept. 1994.

[11] R. Priebbenow, "Triangulation of SPOT Imagery at the Department of Lands, Queensland," in *Test of Triangulation of SPOT Data, Official Publication no. 26*. Frankfurt am Main, Germany: Eur. Org. Experimental Photogramm. Res., 1991, pp. 109–128.

[12] C. V. Tao, Y. Hu, J. B. Mercer, and S. Schnick, "Image rectification using a generic sensor model—rational function model," *Int. Arch. Photogramm. Remote Sensing*, pt. B3, vol. 33, pp. 874–881, 2000.

Changno Lee received the B.A. and M.S. degrees in civil engineering from the Seoul National University, Seoul, Korea, in 1987 and 1989, respectively, and the Ph.D. degree from Purdue University, West Lafayette, IN, in 1999.

He is currently a Postdoctoral Researcher in the Geomatics Area, School of Civil Engineering, Purdue University. His research interests are sensor modeling, computer vision, and automated feature extraction from imagery.

James Bethel received the B.A. degree in mathematics and the M.S. degree in civil engineering, both from the University of Washington, Seattle, in 1974 and 1976, respectively, and the Ph.D. degree from Purdue University, West Lafayette, IN, in 1983.

He has with Teledyne Geotronics doing photogrammetric software development, then Kern Instrument as a Design and Software Engineer, and now works as an Associate Professor in the Geomatics Area, School of Civil Engineering, Purdue University. His research interests are sensor modeling, robust estimation, and automated terrain and feature extraction from imagery.